ACS APPLIED MATERIALS & INTERFACES

Research Article

www.acsami.org

Photoactive PDI–Cobalt Complex Immobilized on Reduced Graphene Oxide for Photoelectrochemical Water Splitting

Janardhan Balapanuru,[†,‡] Gordon Chiu,[‡] Chenliang Su,[†] Na Zhou,[†] Zhu Hai,[†] Qing-hua Xu,[†] and Kian Ping Loh*[,†]

[†]Department of Chemistry and Graphene Research Centre (GRC), National University of Singapore, 3 Science Drive 3, Singapore 117543, Singapore

[‡]Graphite Zero Pte. Ltd., 20 Maxwell Road, #11-18, Maxwell House, Singapore 069113, Singapore

Supporting Information

ABSTRACT: We report the synthesis of a perylene derivative (perylene tetracarboxylic di(propyl imidazole), abbreviated as PDI) that is coordinated with Co(II) ions to form a coordination polymer $[PDI–Co(Cl)_2(H_2O)_2]_n$ (abbreviated as PDI-Co). The PDI-Co complex combines the photoactivity of the perylene dye with the electrocatalytic activity of the "Co(II)" center for photoelectrochemical hydrogen evolution reaction (HER). To improve charge transfer interactions, the PDI-Co complex is immobilized on reduced graphene oxide (rGO) via noncovalent interactions to form the rGO–PDI-Co complex. The composite shows good performance in multiple cycle testing and the turnover number (TON vs Co^{II}) of this hybrid material for hydrogen evolution reaction (754 after 5 h) is considerably higher than previously reported dye-sensitized cobalt-based catalysts.

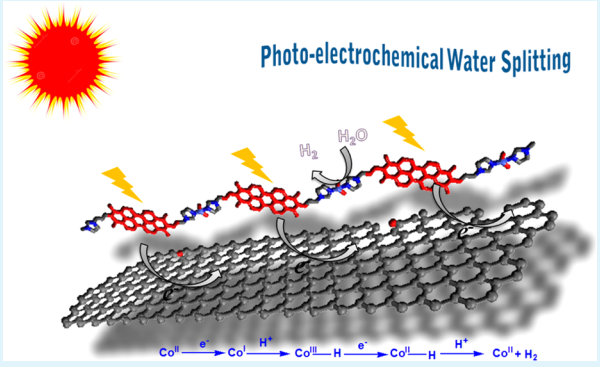

KEYWORDS: *graphene, photoelectrochemical water splitting, hydrogen evolution reaction, perylene, cobalt*

INTRODUCTION

The photoelectrochemical (PEC) splitting of water into hydrogen and oxygen, also known as artificial photosynthesis, affords a way of storing solar energy as hydrogen fuel.[1] A typical PEC consists of an anode (generally *n*-type semiconductor) that absorbs solar energy and converts it into oxidative potential for extracting electrons from water and these electrons are then shuffled to the cathode for hydrogen generation via proton reduction reaction.[2] To increase the efficiency of solar energy conversion, it is desirable to develop a photoactive material that works in the visible region of solar spectrum. Perylene derivatives are useful organic chromospheres for light-driven water splitting systems because of their high molar absorbitivity, stability, inexpensive synthesis and self-assembly properties.[3] For example, the perylene and cobalxime catalyst of Wasielewski et al.[4] forms a donor–acceptor pair whose photoinduced electron transfer ability enables it to show enhanced performance for hydrogen generation.

Compared to molecule-metal "dyads", metal ions coordination polymer networks have attracted great interest because of their intriguing structural diversities and interesting properties such as photoluminescence,[5] magnetism,[6] nonlinear optics,[7] etc. For instance, Würthner et al.[8] reported a photoluminiscent coordination polymer formed from perylene bisimide and Zn(II) ions. Due to their multinuclear absorption and fluorescence properties, they have been investigated for artificial light harvesting systems and other optoelectronic applications.[9]

Herein, we report a cobalt ion-bridged perylene coordination polymer for hydrogen evolution reaction (HER). In general, it is helpful to have an electron mediator to supply the photoinduced electron from the photosensitizer to cobalt catalyst.[4] The aromatic scaffold of reduced graphene oxide (rGO) allows it to act as an efficient electron mediator.[2] Porphyrin immobilized on rGO had been demonstrated to be an efficient catalyst for photosynthetic production of formic acid from CO_2.[10] Several reports, which include Eosin Y/rGO/Pt,[11] graphene–CNT/Fe_2O_3,[12] $BiVO_4$–rGO,[13] and Cu_2O–rGO/Pt,[2] demonstrated the efficiency of rGO as a good electron mediator to enhance the photoelectrocatalytic hydrogen evolution. In this work, we use rGO as the scaffold and electron transfer mediator for the photocatalytic system in water splitting and obtained a turnover number (TON) value that is highly competitive with that of the state-of-the-art system.

Received: October 27, 2014
Accepted: December 15, 2014
Published: December 15, 2014

DOI: 10.1021/am507451c
ACS Appl. Mater. Interfaces 2015, 7, 880–886

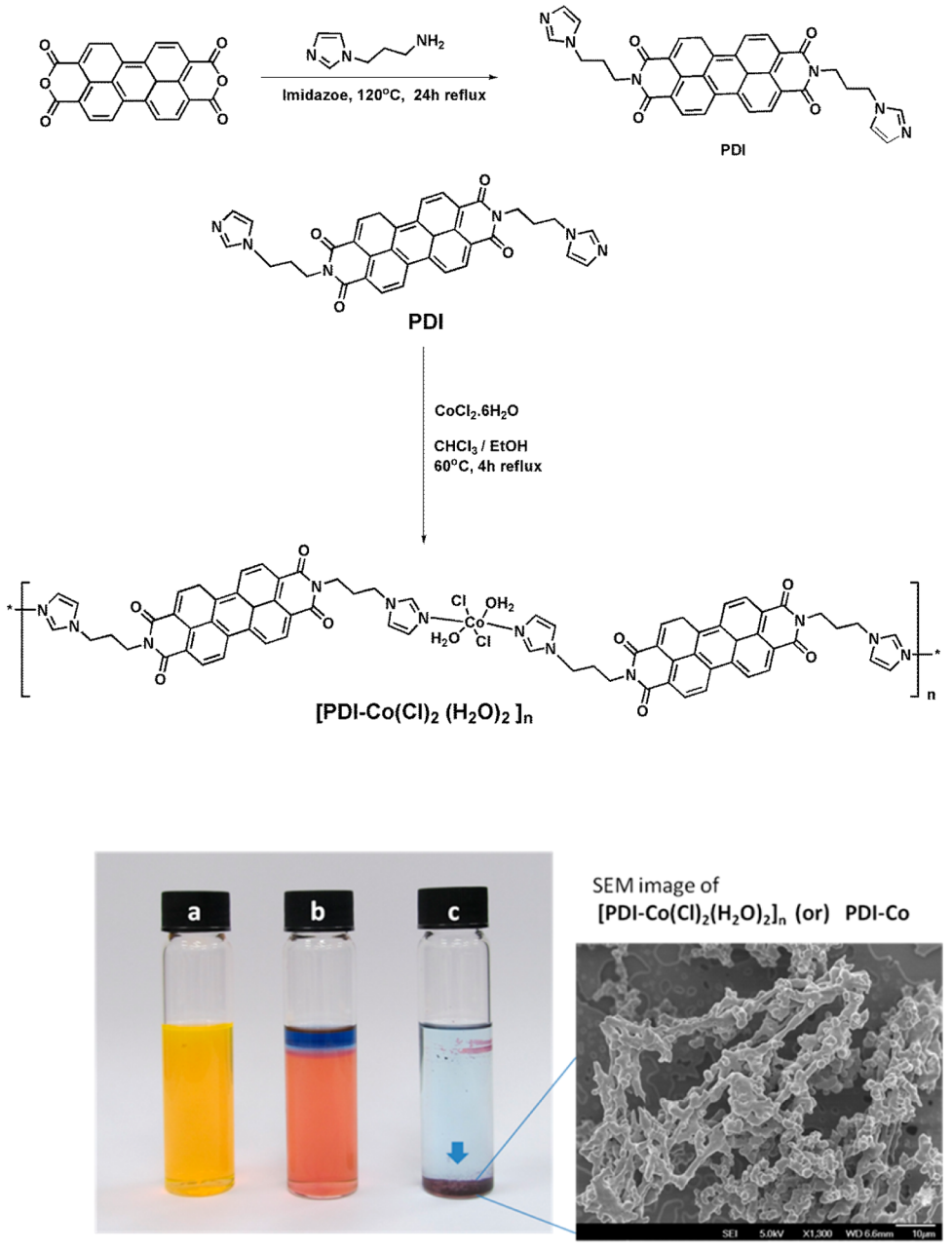

Figure 1. Synthetic route for the coupling of PDI to $CoCl_2$ to form "PDI-Co" polymer. (a) PDI in $CHCl_3$, (b) separation of $CoCl_2{\cdot}6H_2O$ solution on the top of PDI solution (color changed due to diffusion of $CoCl_2$) and (c) after 4 h of heating, formation of "PDI-Co" polymer precipitate (in set is SEM image of final product).

RESULTS AND DISCUSSION

To form a photoactive perylene coordination polymer network, the core perylene is modified with coordination ligands on either side of its core structure. Imidazole derivatives have strong coordinating ability with various metals including Co(II)[19] and Ru(II).[20] Motivated thus, a perylene derivative (perylene tetracarboxylic di(propyl Imidazole) (PDI)) with two imdazole groups on either side of the core perylene moiety is synthesized (see the Supporting Information) from perylene-3,4,9,10-tetracarboxylic dianhydride and a 1-(3-amino propyl) imidazole.[19] When PDI is mixed with $CoCl_2{\cdot}6H_2O$ in 1:1 ratio, two water molecules from $CoCl_2{\cdot}6H_2O$ are exchanged with two imiazole moieties. forming a coordination polymer network $[PDI\text{-}Co(H_2O)_2Cl_2]_n$ or PDI-Co (Figure 1).[19] The coupling between PDI and $CoCl_2{\cdot}6H_2O$ is facile and produces an instantaneous color change from orange to pink. To improve charge-transfer interactions, the PDI-Co is immobilized on reduced graphene oxide (rGO) via noncovalent interactions to form rGO−PDI-Co complex.

UV/vis absorption studies were carried out to probe the photophysical properties and charge transfer interactions of PDI, PDI-Co, rGO and rGO−PDI-Co complexes. As shown in Figure 2, there is a strong absorption for PDI at 485 and 525 nm, which is mainly due to the $\pi-\pi^*$ transitions of the perylene core.[15] When PDI is coordinated to the Co(II) ions, the peak at 525 nm is red-shifted to 580 nm, indicating a strong interactive coupling between PDI and Co(II).[4] The resultant 580 nm peak is further red-shifted upon $\pi-\pi$ stacking on rGO, suggesting electron transfer from PDI-Co to rGO (charge-transfer dynamics will be discussed in subsequent sections in

DOI: 10.1021/am507451c
ACS Appl. Mater. Interfaces 2015, 7, 880−886

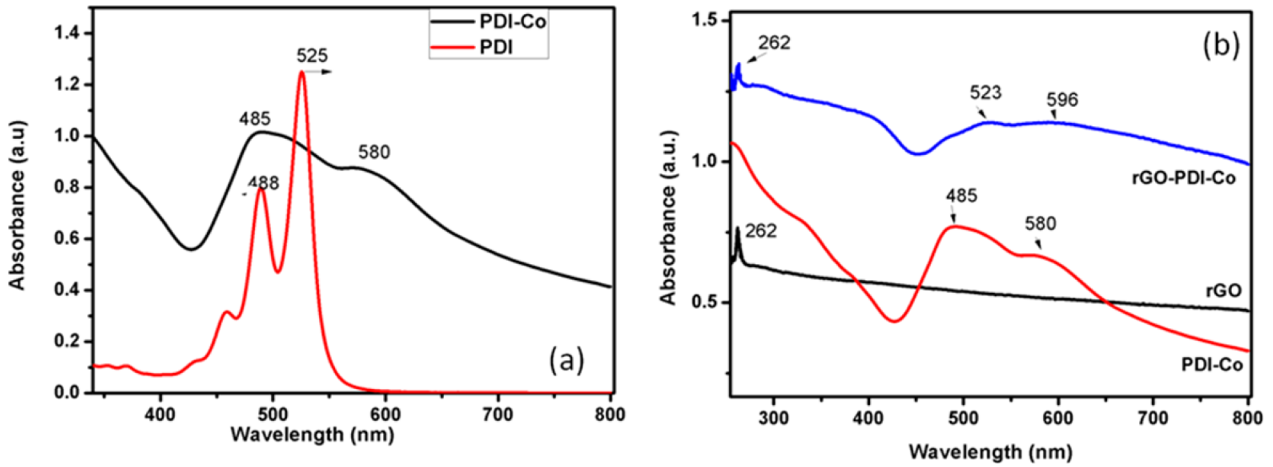

Figure 2. UV−vis absorption Spectra of PDI and PDI-Co and rGO−PDI-Co suspensions in DMF/ethanol mixture. (a) Comparison between PDI and PDI-Co and (b) comparison between PDI-Co, rGO and rGO−PDI-Co.

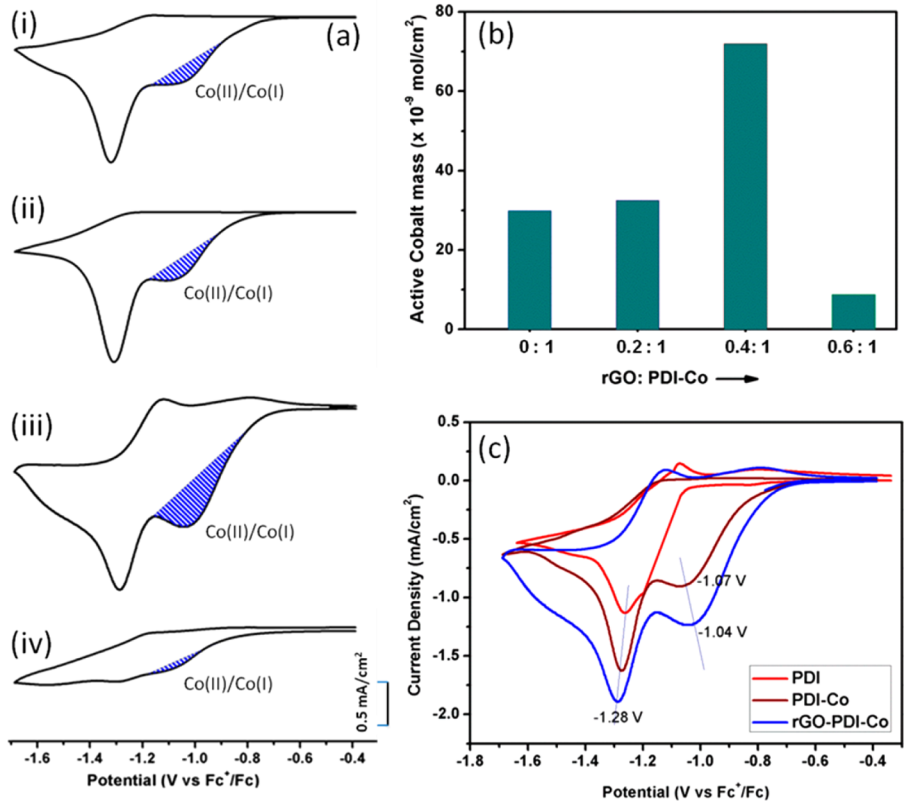

Figure 3. (a) Cyclic voltammogram(CV)s of (i) PDI-Co (ii) rGO:PDI-Co (0.2:1) (iii) rGO:PDI-Co (0.4:1) and (iv) rGO:PDI-Co (0.6:1); all voltammograms were measured in dry acetonitrile (0.1 M nBu4N$^+$PF$_6^-$) at a scan rate of 10 mV·s^{-1}. (b) Active cobalt mass comparison among various composites of rGO/PDI-Co and (c) comparative CV plots of PDI, PDI-Co and rGO−PDI-Co.

Figure 5b).[24] In the composite, the absorption peaks due to PDI-Co overlap with the broad absorption peaks of rGO.[10−14] Overall, a red shift of ∼70 nm (Figure 2) renders this rGO−PDI-Co complex a visible light-responsive material. The characteristic graphene peak at 263 nm (due to $\pi-\pi^*$ transition)[22] serves as an evidence for the presence of rGO in rGO−PDI-Co complex.

Fourier Transform Infrared (FITR) spectroscopic studies also provide further evidence of the chemical structure from the fingerprint peaks of the respective components (Supporting Information, Figure S4). Scanning electron microscopy (SEM) and electron dispersion X-ray spectroscopy (EDS) analyses of PDI-Co show the morphology and the special distribution of C, N, O, Co and Cl elements in the composite. (Supporting Information, Figures S4 and S5). Thermal gravimetric analysis (TGA) characterizations were also carried out to understand the thermal behavior of rGO−PDI-Co (Supporting Information, Figure S6).

The electrochemical behavior of PDI, PDI-Co and rGO−PDI-Co in the dark was investigated. For this, PDI, PDI-Co and rGO−PDI-Co suspensions in ethanol solution were drop-casted and allowed to dry on a platinum disk electrode. Cyclic

DOI: 10.1021/am507451c
ACS Appl. Mater. Interfaces 2015, 7, 880−886

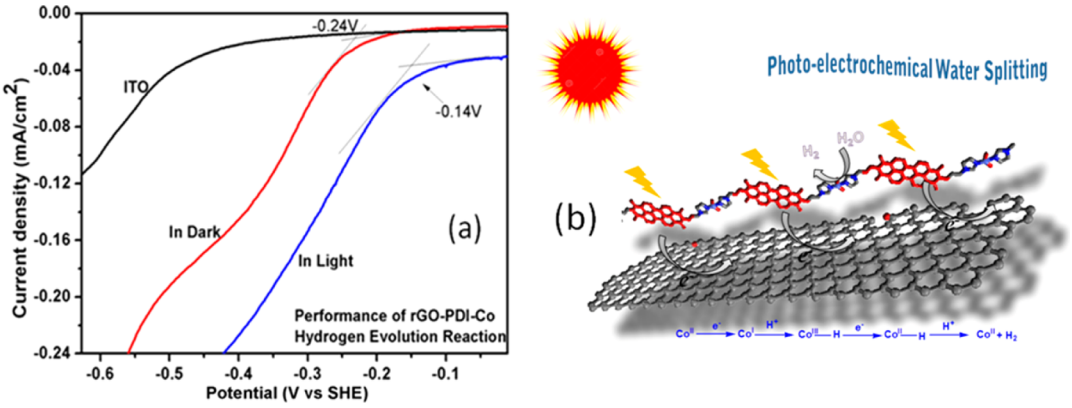

Figure 4. (a) Liner voltammograms (LSV) of rGO−PDI-Co for hydrogen evolution reaction (HER) under visible light illumination (λ > 400 nm) in 1 M phosphate buffer pH 6.8 at scan rate 10 mV s^{-1} and (b) schematic illustion of rGO−PDI-Co working principle.

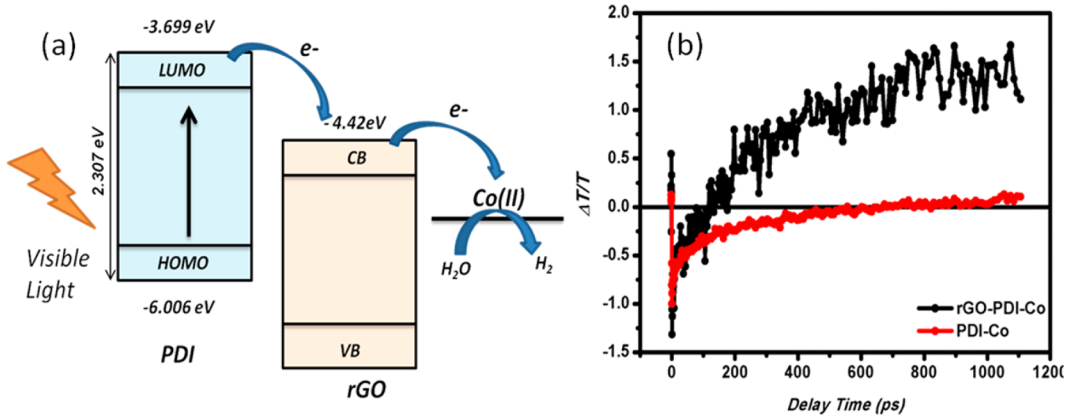

Figure 5. (a) Schematic representation of possible electron transfer processes in rGO−PDI-Co complex for photoelectrochemical hydrogen evolution reaction. (b) Normalized transient absorption of rGO−PDI-Co and PDI-Co solutions monitored at 530 nm with a pulse energy of 20 nJ/pulse.

voltammograms (CV) were recorded using a standard three-electrode electrochemical setup at a scan rate of 10 mV/s (Figure 3c). 0.1 M tetrabutyl ammonium hexafluorophosphate (TBA) in dry acetonitrile was used as the electrolyte. A strong reduction peak at −1.28 V (vs ferrocenium/ferrocene Fc^+/Fc) in Figure 3c corresponds to the reduction of PDI.[15] Upon coupling with the cobalt complex, an additional peak centered at −1.07 V (vs Fc^+/Fc) assignable to the Co(II)/Co(I) redox appears. The reduction potentials of both PDI and Co(II)/Co(I) are in good agreement with the reported values.[24] In the case of rGO−PDI-Co, the corresponding Co(II)/Co(I) peak is shifted slightly toward positive potential (From −1.07 to −1.04 V) whereas the position of the PDI reduction peak is shifted from −1.24 to −1.28 V (vs Fc^+/Fc), which is attributed to the facile electron-transfer mediated by the conductive rGO scaffold.[16−18] (Figure 3c). The current densities of both peaks are larger for rGO−PDI-Co as compared to individual rGO and PDI-Co.

As shown in Figure 3, the active cobalt catalyst concentration in the rGO−PDI-Co sample can be estimated from the integration of the monoelectronic wave at −1.04 V, which is calculated to be 7.21 × 10^{-8} mol·cm^{-2} from Charge $Q = 1/\nu \int_{VO}^{Vf} I(V)\cdot dV$ (see the Supporting Information for details). The concentration of active Co catalyst in the rGO−PDI-Co allows us to calculate the turnover number, which will be discussed in later sections. To enhance the synergetic interaction in the rGO−PDI-Co complex, it is important to optimize the ratio of rGO and PDI-Co. Optimization of different weight compositions (Figure 3a,b) shows that rGO:PDI-Co with a weight ratio of 0.4:1 yields the highest active-Co(II) mass of 72.1 nmol/cm^2 among the composition we have synthesized. Hence, the optimal weight percentage of rGO is 40%, beyond which the performance will decline (Figure 3b).

The photoelectrochemical activity of optimized rGO−PDI-Co (0.4:1) for HER is examined in N_2-saturated 1 M phosphate buffer solution. For this purpose, the rGO−PDI-Co suspension is deposited as a thin film on indium tin oxide (ITO). The linear sweep voltammogram (LSV) is recorded at scan speed of 10 mV s^{-1} under visible light irradiation (300 W xenon lamp with a 400 nm cutoff filter as a visible light source.) The onset potential for HER is observed to shift from −0.24 to −0.14 V for the rGO−PDI-Co complex under illumination (Figure 4a). The onset potential is lower than recently reported CNT−cobalt molecular catalyst[24] which is at −0.35 V (Vs RHE). The photoexcited electrons generated from PDI are captured by rGO in the composite and transferred to the Co(II) center where the protons are reduced to generate hydrogen.[4]

Figure 5a also illustrates electron transfer process in rGO−PDI-Co according to the band gap level. The conduction band level of rGO (−4.42 eV)[11] is lower than the work function of singlet state energy of exited PDI, i.e, 2.31 eV (from Guassian bandgap calculations), thus favoring charge-transfer from PDI to rGO.[11] To investigate the charge transfer within rGO−PDI-

DOI: 10.1021/am507451c
ACS Appl. Mater. Interfaces 2015, 7, 880−886

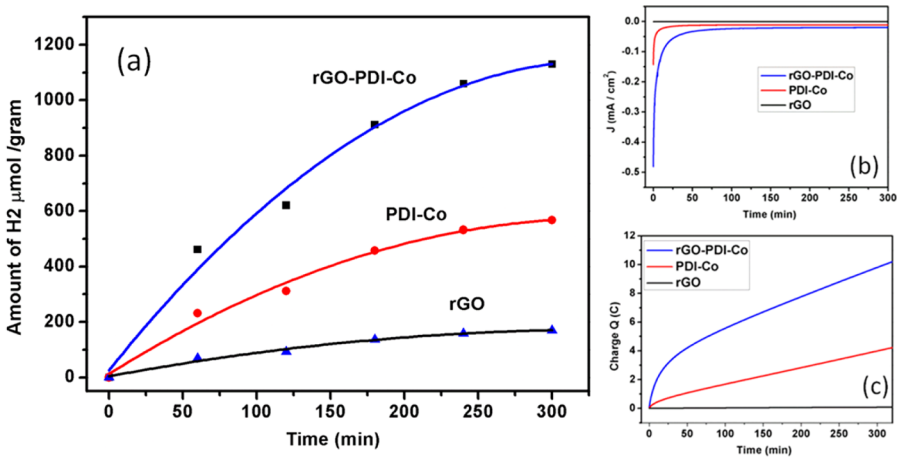

Figure 6. (a) Amount of H_2 evolved from rGO−PDI-Co, rGO PDI-Co and samples illuminated under visible light and at an applied potential of −0.4 V (vs RHE) (5% Triethylamine (TEA) is used as hole scavenger), (b) evolution of the current densities during the photoelectrochemical hydrogen evolution and (c) charge passed during the same experiments.

Co complex, we carried out femtosecond pump−probe experiments.

From Figure 5b, it can be seen that the dynamics of PDI-Co (dye) are dominated by photoabsorption, which originates from the larger absorption cross section of exited state compared to ground state with a relaxation time of 400 ps. No signal was observed for rGO solution under this experimental configuration (see the Supporting Information for experimental details). However, linking PDI-Co to rGO offers an additional route to dissipate the excess exited state energy of dye via ultrafast charge transfer with a decay time of 80 ps. From rGO, the electrons are transferred to the Co(II)−H complex to generate Co(I) and molecular hydrogen as shown below (eq 1).[29−33,35]

$$Co^{II} \xrightarrow{e^-} Co^{I} \xrightarrow{H^+} Co^{III}{-}H \xrightarrow{e^-} Co^{II}{-}H \xrightarrow{H^+} Co^{II} + H_2 \quad (1)$$

Following, HER is quantified using an online gas chromatographic (GC) TCD detector. The evolution of hydrogen gases during the photoelectrochemical water splitting reaction is measured for all samples in 1 M PBS buffer solution at pH 6.8 with an applied bias of −0.4 V vs SHE. Figure 6a shows the photocatalytic H_2 evolution of rGO−PDI-Co under visible light (λ > 400 nm) irradiation. The amount of H_2 evolved from rGO−PDI-Co after 30 min of irradiation is ∼0.4 mmol g^{-1}, which is higher than that produced from PDI-Co and rGO alone (Figure 6a). After 5 h, the amount of hydrogen evolved from rGO−PDI-Co increases to ∼1.2 mmol g^{-1}, which translates to a HER evolution rate of 225 μmol g^{-1} h^{-1}. This performance surpasses that of previously reported photoactive Au doped TiO_2 (50 μmol g^{-1} h^{-1}).[35] We have also investigated the reusability of rGO−PDI-Co in multiple testing cycles (Supporting Information, Figure S7). As shown in the Figure S7 (Supporting Information), even after the 4th cycle test, rGO−PDI-Co is functioning well in terms of H_2 production (Supporting Information, Figure S7).[29] The decrease in the amount of hydrogen produced after 3rd cycle can be attributed to the degradation of PDI-Co under continious irradation (λ > 400 nm) and applied voltage (−0.4 V vs SHE) for >25 h. This is consistent with the previously reported Eosin Y/rGO/Pt,[11] graphene−CNT/Fe_2O_3,[12] $BiVO_4$−rGO[13] and Cu_2O−rGO/Pt[2]

Figure 6b depicts the current densities during the photoelctrochemical hydrogen generation, which can be converted into the charge densities during the process (Figure 6c). Compared to rGO and PDI-Co, the charge density at rGO−PDI-Co is always higher at any given time. For example, the charge density of rGO−PDI-Co reaches ∼10.5 C/cm^2 by 5 h compared to ∼4.5 C/cm^2 observed for PDI-Co.

Considering that two electrons are required for the formation of a H_2 molecule[27] and using the cobalt concentration of 7.21 × 10^{-8} mol·cm^{-2} estimated from CV studies, we can calculate the turnover number (TON vs Co^{II}) of rGO−PDI-Co to be ∼754 after 5 h of operation (see the Supproting Information for details). The TON of rGO−PDI-Co (TON ∼754 vs Co^{II} after 5 h) is higher than that of reported dye-sensitized cobalt catalysts for HER. For example, the ruthenium-based photosensitizer ($[Ru(bpy)_3]^{2+}$) coupled with $[Co(bpy)_3]^{2,36}$ shows a TON of ∼52 and the $[Ir(ppy)^{2-}(bpy)]^{+}$/ $[Co(bpy)_3]^{2+37}$ system shows a TON of ∼42 (vs Co^{II}).[37] Recently, it is highlighted that xanthene dye-coupled $[Co(dmgBF_2)_2(H_2O)_2]$ can give a TON of 212 vs $Co^{(II)}$. The enhanced performance of rGO−PDI-Co[37] composite can be attributed to the higher photostability of perylene dye and the conductive nature of rGO that helps to transfer electrons from the photoexcited PDI to Co(II) in the reduction of H^+ to H_2.[36,37]

CONCLUSIONS

A perylene−cobalt coordination polymer (PDI-Co(II)) was successfully synthesized and coupled to reduced graphene oxide (rGO) via noncovalent interactions to form a catalytically active composite for HER. A strong red shift of 70 nm in absorption peak of PDI provides the evidence for strong charge transfer interactions between rGO and PDI-Co. Synergistic interaction between rGO and PDI-Co(II) polymer promotes charge-transfer and photocatalysis and enhances the hydrogen yield of the photoelectrochemical water spitting reaction significantly compared to control samples. The TON (vs Co^{II}) of rGO−PDI-Co reaches 754 after 5 h of photocatalyzed water splitting and the composite shows good reusability properties. This work demonstrates that interfacing coordination polymer with rGO can generate a highly effective photoelectrochemical platform, which may be potentially applied in wide ranging catalysis reactions.[10]

DOI: 10.1021/am507451c
ACS Appl. Mater. Interfaces 2015, 7, 880−886

■ ASSOCIATED CONTENT

Supporting Information

Synthesis of PDI, PDI-Co, rGO and rGO−PDI-Co composites, electrode preparation, HER-recycle tests and other photoelectrochemical experiments, additional characterizations such as FTIR, SEM, EDS, TGA, MALDI-TOF and description of pump−probe experiments. This material is available free of charge via the Internet at http://pubs.acs.org.

■ AUTHOR INFORMATION

Corresponding Author

*K. P. Loh. E-mail: chmlohkp@nus.edu.sg.

Notes

The authors declare no competing financial interest.

■ ACKNOWLEDGMENTS

Funding support from the Singapore-Berkeley Research Initiative for Sustainable Energy (SinBeRISE) CREATE Program and from Graphite Zero (Singapore) Pte, Ltd. is acknowledged.

■ REFERENCES

(1) Fujishima, A.; Honda, K. Electrochemical Photolysis of Water at a Semiconductor Electrode. *Nature* **1972**, *238*, 37−38.

(2) Tran, P. D.; Batabyal, S. K.; Pramana, S. S.; Barber, J.; Wong, L. H.; Loo, S. C. J. A Cuprous oxide−reduced Graphene oxide (Cu_2O−rGO) Composite Photocatalyst for Hydrogen Generation: Employing rGO as an Electron Acceptor to Enhance the Photocatalytic Activity and Stability of Cu_2O. *Nanoscale* **2012**, *4*, 3875−3878.

(3) Vagnini, M. T.; Smeigh, A. L.; Blakemore, J. D.; Eaton, S. W.; Schley, N. D.; D'Souza, F.; Crabtree, R. H.; Brudvig, G. W.; Co, D. T.; Wasielewski, M. R. Ultrafast Photodriven Intramolecular Electron Transfer from an Iridium-based Water-Oxidation Catalyst to Perylene Diimide Derivatives. *Proc. Nat. Acad. Sci. U. S. A.* **2012**, *109*, 15651−15656.

(4) Veldkamp, B. S.; Han, W.-S.; Dyar, S. M.; Eaton, S. W; Ratner, M. A.; Wasielewski, M. R. Photoinitiated Multi-Step Charge Separation and Ultrafast Charge Transfer Induced Dissociation in a Pyridyl-Linked Photosensitizer−Cobaloxime Assembly. *Energy Environ. Sci.* **2013**, *6*, 1917−1928.

(5) Zou, R.-Q.; Zhong, R.-Q.; Du, M.; Pandey, D. S.; Xu, Q. Controllable Congregating of Homochiral and Achiral Coordination Polymers: Cadmium(II) Pyridine-2,4,6-tricarboxylate Species with Double-Helical Strand and Molecular Building Block Structures. *Cryst. Growth Des.* **2008**, *8*, 452−459.

(6) Zeng, Y.-F.; Hu, X.; Liu, F.-C.; Bu, X.-H. Azido-Mediated Systems Showing Different Magnetic Behaviors. *Chem. Soc. Rev.* **2009**, *38*, 469−480.

(7) Cariati, E.; Macchi, R.; Roberto, D.; Ugo, R.; Galli, S.; Casati, N.; Macchi, P.; Sironi, A.; Bogani, L.; Caneschi, A.; Gatteschi, D. Polyfunctional Inorganic−Organic Hybrid Materials: An Unusual Kind of NLO Active Layered Mixed Metal Oxalates with Tunable Magnetic Properties and Very Large Second Harmonic Generation. *J. Am. Chem. Soc.* **2007**, *129*, 9410−9420.

(8) Dobrawa, R.; Lysetska, M.; Ballester, P.; Grüne, M.; Würthner, F. Fluorescent Supramolecular Polymers: Metal Directed Self-Assembly of Perylene Bisimide Building Blocks. *Macromolecules* **2005**, *38*, 1315−1325.

(9) Stepanenko, V.; Stocker, M.; Muller, P.; Buchner, M.; Wurthner, F. Self-Assembly and Layer-by-Layer Deposition of Metallosupramolecular Perylene Bisimide Polymers. *J. Mater. Chem.* **2009**, *19*, 6816−6826.

(10) Yadav, R. K.; Baeg, J.-O.; Oh, G. H.; Park, N.-J.; Kong, K.-j.; Kim, J.; Hwang, D. W.; Biswas, S. K. A Photocatalyst−Enzyme Coupled Artificial Photosynthesis System for Solar Energy in Production of Formic Acid from CO_2. *J. Am. Chem. Soc.* **2012**, *134*, 11455−11461.

(11) Mou, Z.; Dong, Y.; Li, S.; Du, Y.; Wang, X.; Yang, P.; Wang, S. Eosin Y Functionalized Graphene for Photocatalytic Hydrogen Production from Water. *Int. J. Hydrogen Energy* **2011**, *36*, 8885−8893.

(12) Young Kim, J.; Jang, J.-W.; Hyun Youn, D.; Yul Kim, J.; Sun Kim, E.; Sung Lee, J. Graphene−Carbon Nanotube Composite as an Effective Conducting Scaffold to Enhance the Photoelectrochemical Water Oxidation Activity of a Hematite Film. *RSC Adv.* **2012**, *2*, 9415−9422.

(13) Ng, Y. H.; Iwase, A.; Kudo, A.; Amal, R. Reducing Graphene Oxide on a Visible-Light BiVO4 Photocatalyst for an Enhanced Photoelectrochemical Water Splitting. *J. Phys. Chem. Lett.* **2010**, *1*, 2607−2612.

(14) Hummers, W. S.; Offeman, R. E. Preparation of Graphitic Oxide. *J. Am. Chem. Soc.* **1958**, *80*, 1339−1339.

(15) Keerthi, A.; Valiyaveettil, S. Regioisomers of Perylenediimide: Synthesis, Photophysical, and Electrochemical Properties. *J. Phys. Chem. B* **2012**, *116*, 4603−4614.

(16) Cárdenas-Jirón, G. I.; Leon-Plata, P.; Cortes-Arriagada, D.; Seminario, J. M. Electrical Characteristics of Cobalt Phthalocyanine Complexes Adsorbed on Graphene. *J. Phys. Chem. C* **2011**, *115*, 16052−16062.

(17) Yang, J.; Gao, Y.; Zhang, W.; Tang, P.; Tan, J.; Lu, A.; Ma, D. Cobalt Phthalocyanine−Graphene Oxide Nanocomposite: Complicated Mutual Electronic Interaction. *J. Phys. Chem. C* **2013**, *117*, 3785−3788 and.

(18) Rostalski, J.; Giebeler, C.; Martin, S. J.; Bradley, D. D. C.; Meissner, D. Electroabsorption studies of phthalocyanine/perylene solar cells. *Sol. Energy Mater. Sol. Cells* **2000**, *63*, 3−13.

(19) Atria, A. M.; Cortes, P.; Garland, M. T.; Baggio, R. Two Isomorphous Imidazole (Him) Complexes: $[Mcl_2(Him)_2(H_2O)_2]$ (M = Co and Ni). *Acta Crystallogr.* **2003**, *59*, m396−m398.

(20) Reddy, K. B.; Cho, M.-o. P.; Wishart, J. F.; Emge, T. J.; Isied, S. S. cis-Bis(bipyridine)ruthenium Imidazole Derivatives: A Spectroscopic, Kinetic, and Structural Study. *Inorg. Chem.* **1996**, *35*, 7241−7245.

(21) Balapanuru, J.; Yang, J.-X.; Xiao, S.; Bao, Q.; Jahan, M.; Polavarapu, L.; Wei, J.; Xu, Q.-H.; Loh, K. P. A Graphene Oxide−Organic Dye Ionic Complex with DNA-Sensing and Optical-Limiting Properties. *Angew. Chem., Int. Ed.* **2010**, *49*, 6549−6553.

(22) Jahan, M.; Bao, Q.; Yang, J.-X.; Loh, K. P. Structure-Directing Role of Graphene in the Synthesis of Metal−Organic Framework Nanowire. *J. Am. Chem. Soc.* **2010**, *132*, 14487−14495.

(23) Su, C.; Acik, M.; Takai, K.; Lu, J.; Hao, S.-j.; Zheng, Y.; Wu, P.; Bao, Q.; Enoki, T.; Chabal, Y. J.; Loh, K. P. Probing The Catalytic Activity of Porous Graphene Oxide and the Origin of this Behaviour. *Nat. Commun.* **2012**, *3*, 1298.

(24) Navarro, C. U.; Machado, F.; López, M.; Maspero, D.; Perez-Pariente, J. A SEM/EDX Study of the Cobalt Distribution in CoAPO-Type Materials. *Zeolites* **1995**, *15*, 157−163.

(25) Koyuncu, S.; Kus, M.; Demic, S.; Kaya, İ.; Ozdemir, E.; Icli, S. Electrochemical and Optical Properties of Novel Donor-Acceptor Thiophene-Perylene-Thiophene Polymers. *J. Poly. Sci. Part A: Polym. Chem.* **2008**, *46*, 1974−1989.

(26) Moore, G. F.; Blakemore, J. D.; Milot, R. L.; Hull, J. F.; Song, H.-e.; Cai, L.; Schmuttenmaer, A.; Crabtree, R. H.; Brudvig, G. W. A Visible Light Water-Splitting Cell With a Photoanode Formed by Codeposition of a High-Potential Porphyrin and an Iridium Water-Oxidation Catalyst. *Energy Environ. Sci.* **2011**, *4*, 2389−2392.

(27) Andreiadis, E. S.; Jacques, P.-A.; Tran, P. D.; Leyris, A.; Chavarot-Kerlidou, M.; Jousselme, B.; Matheron, M.; Pécaut, J.; Palacin, S.; Fontecave, M.; Artero, V. Molecular Engineering of a Cobalt-based Electrocatalytic Nanomaterial for H_2 Evolution under Fully Aqueous Conditions. *Nat. Chem.* **2013**, *5*, 48−53.

(28) Kalu, E. E.; Nwoga, T. T.; Srinivasan, V.; Weidner, J. W. Cyclic Voltammetric Studies of the Effects of Time and Temperature on the Capacitance of Electrochemically Deposited Nickel Hydroxide. *J. Power Sources* **2001**, *92*, 163−167.

DOI: 10.1021/am507451c
ACS Appl. Mater. Interfaces 2015, 7, 880−886

(29) Singh, W. M.; Baine, T.; Kudo, S.; Tian, S.; Ma, X. A. N.; Zhou, H.; DeYonker, N. J.; Pham, T. C.; Bollinger, J. C.; Baker, D. L.; Yan, B.; Webster, C. E.; Zhao, X. Electrocatalytic and Photocatalytic Hydrogen Production in Aqueous Solution by a Molecular Cobalt Complex. *Angew. Chem., Int. Ed.* **2012**, *51*, 5941−5944.
(30) Dempsey, J. L.; Brunschwig, B. S.; Winkler, J. R.; Gray, H. B. Hydrogen Evolution Catalyzed by Cobaloximes. *Acc. Chem. Res.* **2009**, *42*, 1995−2004.
(31) Lazarides, T.; McCormick, T.; Du, P.; Luo, G.; Lindley, B.; Eisenberg, R. Making Hydrogen from Water Using a Homogeneous System Without Noble Metals. *J. Am. Chem. Soc.* **2009**, *131*, 9192−9194.
(32) McCormick, T. M.; Calitree, B. D.; Orchard, A.; Kraut, N. D.; Bright, F. V.; Detty, M. R.; Eisenberg, R. Reductive Side of Water Splitting in Artificial Photosynthesis: New Homogeneous Photosystems of Great Activity and Mechanistic Insight. *J. Am. Chem. Soc.* **2010**, *132*, 15480−15483.
(33) Latorre-Sánchez, M.; Lavorato, C.; Puche, M.; Fornés, V.; Molinari, R.; Garcia, H. Visible-Light Photocatalytic Hydrogen Generation by Using Dye-Sensitized Graphene Oxide as a Photocatalyst. *Chem.—Eur. J.* **2012**, *18*, 16774−16783.
(34) Kim, E. S.; Nishimura, N.; Magesh, G.; Kim, J. Y.; Jang, J.-W.; Jun, H.; Kubota, J.; Domen, K.; Lee, J. S. Fabrication of $CaFe_2O_4$/TaON Heterojunction Photoanode for Photoelectrochemical Water Oxidation. *J. Am. Chem. Soc.* **2013**, *135*, 5375−5383.
(35) Probst, B.; Kolano, C.; Hamm, P.; Alberto, R. An Efficient Homogeneous Intermolecular Rhenium-based Photocatalytic System for the Production of H_2. *Inorg. Chem.* **2009**, *48*, 1836−1843.
(36) Dong, J.; Wang, M.; Zhang, P.; Yang, S.; Liu, J.; Li, X.; Sun, L. Promoting Effect of Electrostatic Interaction between a Cobalt Catalyst and a Xanthene Dye on Visible-Light-Driven Electron Transfer and Hydrogen Production. *J. Phys. Chem. C* **2011**, *115*, 15089−15096.
(37) Takizawa, S.-y.; Pérez-Bolívar, C.; Anzenbacher, P.; Murata, S. Cationic Iridium Complexes Coordinated with Coumarin Dyes − Sensitizers for Visible-Light-Driven Hydrogen Generation. *Eur. J. Inorg. Chem.* **2012**, *2012*, 3975−3979.

DOI: 10.1021/am507451c
ACS Appl. Mater. Interfaces 2015, 7, 880−886